Available online at www.sciencedirect.com
SCIENCE DIRECT
Journal of Catalysis 235 (2005) 262–271
JOURNAL OF CATALYSIS
www.elsevier.com/locate/jcat

The effect of Ni in Pd–Ni/(Ce,Zr)O_x/Al_2O_3 catalysts used for stoichiometric CO and NO elimination. Part 2: Catalytic activity and in situ spectroscopic studies

A.B. Hungría [a], M. Fernández-García [a], J.A. Anderson [b], A. Martínez-Arias [a,*]

[a] *Instituto de Catálisis y Petroleoquímica, CSIC, C/ Marie Curie, Campus Cantoblanco, 28049 Madrid, Spain*
[b] *Surface Chemistry and Catalysis Group, Department of Chemistry, University of Aberdeen, AB24 3UE Scotland, UK*

Received 18 March 2005; revised 30 June 2005; accepted 16 August 2005

Abstract

Pd–Ni catalysts supported on Al_2O_3, (Ce,Zr)O_x/Al_2O_3, and (Ce,Zr)O_x were examined with the principle objective of determining the effects of Ni on catalytic activity for CO oxidation and NO reduction reactions under stoichiometric conditions. Catalytic activity findings for the CO + O_2 and CO + O_2 + NO reactions were analyzed in conjunction with in situ DRIFTS and XANES results to obtain information on the processes occurring in the catalysts during the course of the reactions. The results reveal a significant dependence on the nature of the support in terms of the catalytic changes produced by nickel. In the absence of significant nickel-induced electronic perturbations of palladium, these are related to indirect effects on palladium distribution over the catalysts or to a certain impediment of the interactions between active palladium and Ce–Zr mixed-oxide components. Significant promotion of CO oxidation was observed for the (Ce,Zr)O_x/Al_2O_3-supported catalyst, which reveals a relevant role for the particle size of the nanostructured Ce–Zr mixed oxide in this reaction.

Keywords: Pd–Ni catalysts; TWC; CeO_2–ZrO_2; Al_2O_3; CO oxidation; NO reduction; DRIFTS; Pd *K*-edge XANES

1. Introduction

Part 1 of this work was dedicated to analyzing in detail aspects of characterization that could be relevant to understanding the catalytic properties of bimetallic Pd–Ni catalysts supported on Al_2O_3, (Ce,Zr)O_x/Al_2O_3, and (Ce,Zr)O_x [1]. These can be related to the amount and nature of the contacts established between Pd and the different support components, the structural and compositional characteristics of the Ce–Zr mixed-oxide component of the support, the dispersion and chemical state of palladium, or the existence of interactions between Pd and Ni [2–12]. In this respect, as we concluded in Part 1 [1], the presence of rather homogeneous Ce–Zr mixed-oxide nanostructures (with average particle sizes of 3.4 and 5.4 nm, respectively) was revealed in (Ce,Zr)O_x/Al_2O_3- and (Ce,Zr)O_x-supported catalysts. The presence of nickel apparently favors a preferential interaction of palladium with the Ce–Zr mixed-oxide component of the support in the (Ce,Zr)O_x/Al_2O_3-supported system, whereas nickel interacts preferentially with the alumina component. Concerning the chemical nature of palladium and nickel components in the initial catalysts, these are shown to appear in the form of small PdO-type or NiO-type particles (in addition, for alumina-supported samples, a part of the nickel can form $NiAl_2O_4$-type particles). Overall, the results suggest no strong interactions between Pd and Ni in the initial calcined systems, although a certain degree of interaction between both components in the (Ce,Zr)O_x-supported catalyst cannot be discounted. The dispersion of palladium and the corresponding characteristic size of the PdO particles were strongly influenced by the support nature. These findings appear to be fairly similar for systems having alumina as the carrier (Al_2O_3- and (Ce,Zr)O_x/Al_2O_3-supported systems), in which particle size averaged ca. 2.5 nm. In contrast, a considerably higher degree

* Corresponding author.
E-mail address: amartinez@icp.csic.es (A. Martínez-Arias).

0021-9517/$ – see front matter
doi:10.1016/j.jcat.2005.08.012

of dispersion was seen in the (Ce,Zr)O_x-supported catalyst. In turn, nickel achieved highly dispersed states in all of the systems.

This second part of the study aims to analyze the catalytic properties of such Pd–Ni systems, focusing in particular on the promoting effects induced by the presence of nickel in the catalyst formulation. For this purpose, the catalytic activity for CO oxidation and NO reduction of the bimetallic Pd–Ni catalysts supported on Al_2O_3, (Ce,Zr)O_x/Al_2O_3, and (Ce,Zr)O_x during light-off tests was examined in comparison with that of monometallic Pd systems, which have been analyzed in detail in previous studies [7,9,10]. The present study is complemented by the analysis of the catalysts under reaction conditions by in situ DRIFTS and XANES techniques to obtain information on possible changes occurring during the course of the reaction on interaction with the reactant mixture.

2. Experimental

The catalysts were prepared as indicated in Part 1 [1]. The bimetallic Pd–Ni catalysts are referred to as PdNiA, PdNiCZA, and PdNiCZ (with 1 wt% loading for each of the metals) for the systems supported on Al_2O_3, $CeZrO_4$/Al_2O_3 (with 10 wt% of the Ce–Zr mixed oxide), and $CeZrO_4$, respectively. Another two bimetallic catalysts with 0.5 and 2 wt% Ni and the same Pd loading (1 wt%) over the CZA support were prepared by the same methods described in Part 1 [1] and are denoted here by Pd0.5NiCZA and Pd2NiCZA, respectively. Monometallic reference catalysts (with 1 wt% loading in all cases) are identified with either Pd or Ni as a prefix.

Catalytic activity tests using stoichiometric gas mixtures of 1% CO + 0.5% O_2 or 1% CO + 0.45% O_2 + 0.1% NO (N_2 balance) at 3×10^4 h^{-1} were performed in a Pyrex glass fixed-bed flow reactor. Space velocity (3×10^4 h^{-1}) and sieving size (particles in the 0.125–0.250 mm range) were selected to minimize diffusion effects [13] as estimated from independent tests performed on the PdNiCZA catalyst for the CO–O_2 reaction, which indicated the absence of significant mass-transfer limitations for particle sizes < ca. 0.5 mm (at least for conversion values < ca. 50% in this case); in this respect and for comparative purpose, it is worth noting that no significant differences in textural properties (surface area, pore distribution) were detected when comparing monometallic Pd and bimetallic Pd–Ni catalysts on each respective support. The gases used (all of commercial purity: 99.9% CO, 99.99% O_2, and 98.5% NO, the latter with 1% NO_2 and 0.5% N_2O as the main impurities) were regulated with mass flow controllers and analyzed on-line using a Perkin–Elmer 1725X Fourier transform infrared (FTIR) spectrometer coupled with a multiple reflection transmission cell (Infrared Analysis Inc.). Oxygen concentrations were determined using a paramagnetic analyzer (Servomex 540A). Experimental error in the CO and/or NO conversion values obtained under these conditions is estimated as ±7%. Before catalytic testing, a calcination pretreatment was performed in situ under 2.5% O_2 (in N_2) at 773 K, followed by cooling under the same atmosphere and a thorough N_2 purge at room temperature. Tests were performed in the light-off mode, increasing the temperature under the reactive flow at a ramp rate of 5 K min^{-1}, with a glass-sheathed thermocouple placed in the center of the catalyst bed for temperature control.

Diffuse reflectance infrared Fourier transform spectroscopy (DRIFTS) analysis of adsorbed species present on the catalyst surface under reaction conditions was carried out using a Perkin–Elmer 1750 FTIR fitted with an MCT detector. On-line analysis of the NO concentration at the outlet of the infrared (IR) chamber was performed by chemiluminescence (Thermo Environmental Instruments 42C). The DRIFTS cell (Harrick) was fitted with CaF_2 windows and a heating cartridge that allowed samples to be heated to 773 K. Samples of ca. 65 mg were pretreated in situ under diluted O_2 (in a manner similar to that for the catalytic tests), before introduction of the reaction mixture and heating at 2 K min^{-1} from 298 to 673 K, recording one spectrum (4 cm^{-1} resolution, average of 50 scans) generally every 10–15 K. The gas mixture (similar to that used for catalytic tests) was prepared using a computer-controlled gas blender with 80 cm^3 min^{-1} passing through the catalyst bed.

X-Ray absorption near-edge structure (XANES) experiments at the Pd *K*-edge were performed on beamline BM29 of the ESRF synchrotron and at station 9.3 of the SRS synchrotron. A Si(311) double-crystal monochromator was used in conjunction with a rejection mirror to minimise the harmonic content of the beam. Transmission experiments were carried out using Kr/Ar-filled ionization chambers. The energy scale was simultaneously calibrated by measuring a Pd foil using a third ionization chamber. Samples were self-supported (absorbance, 0.5–1.0) and placed in a controlled-atmosphere cell for treatment. XANES spectra were taken every 15 K in the presence of the CO + NO + O_2 flowing mixture (similar to the one used for catalytic activity tests) during a 5 K min^{-1} temperature ramp up to 673 K. The series of spectra were analyzed using principal factor analysis (PCA), details of which can be found elsewhere [14].

Further analysis of the catalysts after use in the catalytic tests mentioned earlier was performed by X-ray diffraction, using the equipment described in Part 1 [1]. The diffractograms obtained were analogous to those observed for the initial calcined catalysts, thus revealing the stability of the support components under reaction conditions [1].

3. Results

3.1. Catalytic activity tests

Fig. 1 shows the conversion profiles obtained for the bimetallic catalysts under CO + O_2. The results demonstrate the promoting role of the Ce–Zr mixed-oxide component, in accordance with results reported previously for the monometallic Pd catalysts [9]. Relatively low apparent activation energies, in the 25–35 kJ mol^{-1} range (which should be considered only in qualitative terms, because the high activity of the catalysts at room temperature precludes a guarantee of the system's differential behavior), are estimated from analysis of low conversion points of PdNiCZ and PdNiCZA catalysts, suggesting active sites involving palladium–cerium contacts [15]. Greater promo-

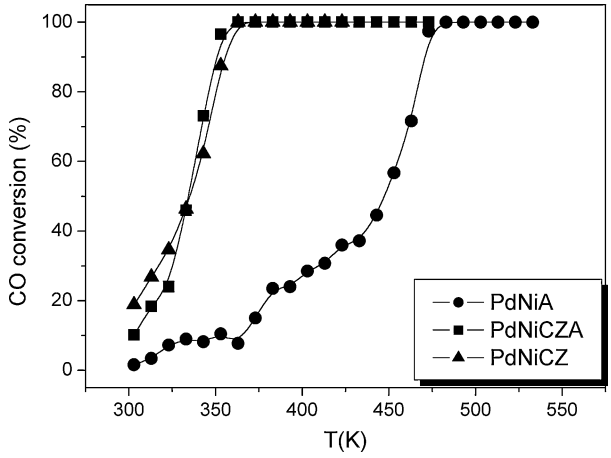

Fig. 1. CO conversion profiles obtained during the CO–O_2 reaction over the indicated catalysts.

Table 1
Isoconversion temperatures (in K) at 50% conversion obtained during stoichiometric CO–O_2 and CO–O_2–NO reactions (3×10^4 h^{-1} GHSV) over the bimetallic Pd–Ni catalysts and the corresponding monometallic references

Sample	$T_{50}CO_{CO+O_2}$			$T_{50}CO_{CO+NO+O_2}$			$T_{50}NO_{CO+NO+O_2}$		
	PdNi	Pd	Ni	PdNi	Pd	Ni	PdNi	Pd	Ni
A-supported	447	447		479	479		408	410	
CZA-supported									
0.5 wt% Ni	334			406			460		
1 wt% Ni	334	404	637	403	433	668	455	456	770
2 wt% Ni	339			410			464		
CZ-supported	335	<303	498	356	358	520	448	485	>773

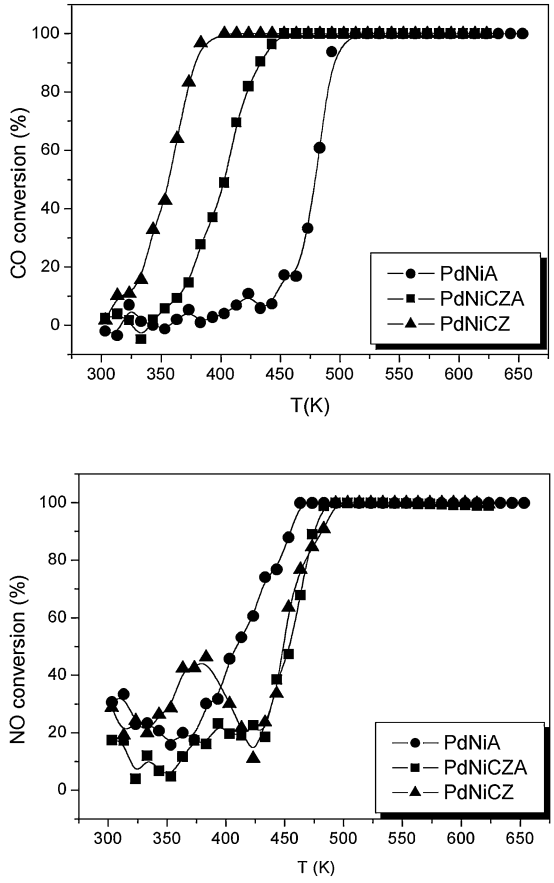

Fig. 2. Conversion profiles obtained during the CO–O_2–NO reaction over the indicated catalysts.

tion of CO oxidation activity was achieved in the presence of Ni for the CZA-supported catalyst, as evidenced by data presented in Table 1. These data reveal an important promoting effect of nickel in this system that appears to be almost independent of the amount of nickel present in the catalyst (Table 1). In contrast, the presence of Ni produced an apparent decrease in CO oxidation activity in the CZ-supported system, but had no significant influence on the A-supported system (Table 1).

Different effects were induced by the presence of NO in the reactant mixture as a function of the support and/or the presence of Ni in the catalyst (Fig. 2; Table 1). The only material for which the presence of Ni did not appear to exert any significant influence was the A-supported catalyst, which in turn displayed the greatest NO reduction activity. As observed previously for the monometallic Pd catalysts [7,10], the presence of NO had a detrimental effect on CO oxidation activity in the bimetallic systems. However, in contrast to the behavior observed for the monometallic systems for which the magnitude of the NO-induced reduction of the CO oxidation activity was observed to increase with the CZ content of the catalyst [10], a relatively greater level of deactivation was observed here for PdNiCZA than for PdNiCZ. In terms of NO reduction, the results reveal that the presence of Ni somewhat limited the detrimental effect induced by the establishment of Pd–CZ contacts [10]. This Ni-induced enhancement of NO reduction activity was particularly pronounced for the PdNiCZ system (Table 1). In contrast, no specific influence of the presence of Ni could be identified in overall terms in regard to N_2 selectivity in the NO reduction process, in accordance with previous reports [7,10]). Other details apparent in the NO conversion profiles shown in Fig. 2 concern the presence of oscillations at relatively low reaction temperatures (particularly for the CZ-supported system), which, in accordance with previous analyses [10], are essentially related to adsorption/desorption of NO_x species. Additionally, analysis of the data in Table 1 reveals that changing the Ni loading (in the 0.5–2.0 wt% range) in the bimetallic CZA-supported system produced only minimal effects on the catalytic activity for these reactions, with the optimum properties achieved in global terms for the 1 wt% Ni system (PdNiCZA). In contrast, comparison with the catalytic performance observed over monometallic Ni systems (Table 1) indicates that the catalytic behavior observed in the bimetallic catalysts cannot be attributed to effects induced by Ni alone.

3.2. *In situ DRIFTS*

The results of DRIFTS experiments recorded under $CO + O_2$ and $CO + O_2 + NO$ for the bimetallic systems are shown in Figs. 3 and 4, respectively. A reasonable correlation is observed between evolution of bands due to gaseous CO_2 (appearing in the 2400–2300 cm^{-1} range) and CO conversion in the catalytic tests (Figs. 1 and 2). Unfortunately, the relatively low

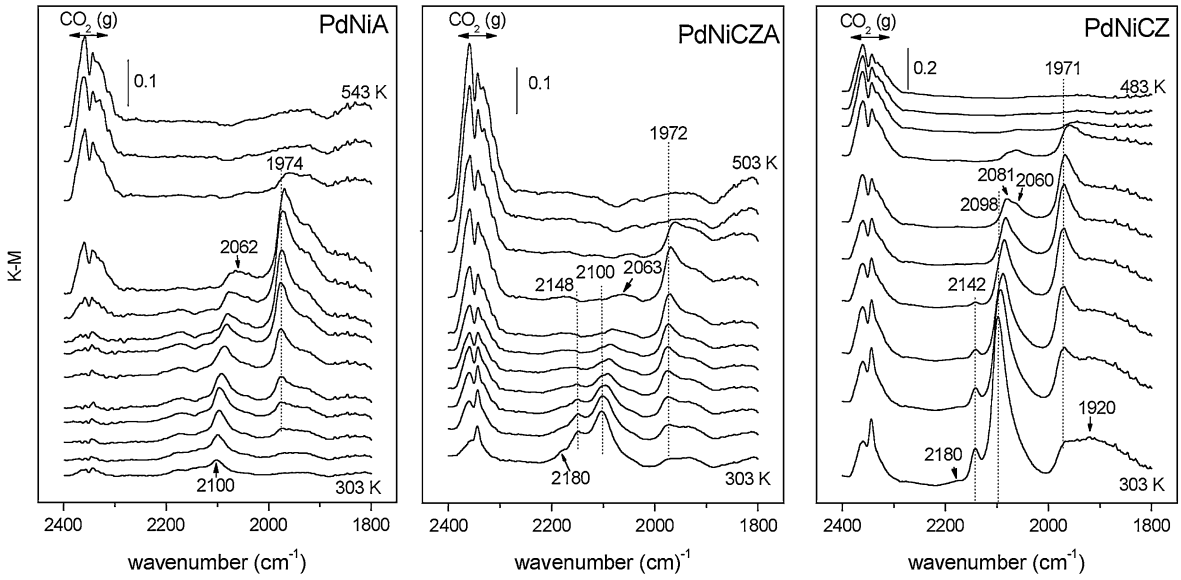

Fig. 3. In situ DRIFTS spectra obtained during the course of the CO–O_2 reaction for the indicated catalysts. Spectra taken every 20 K from 303 up to 483–543 K (from bottom to top).

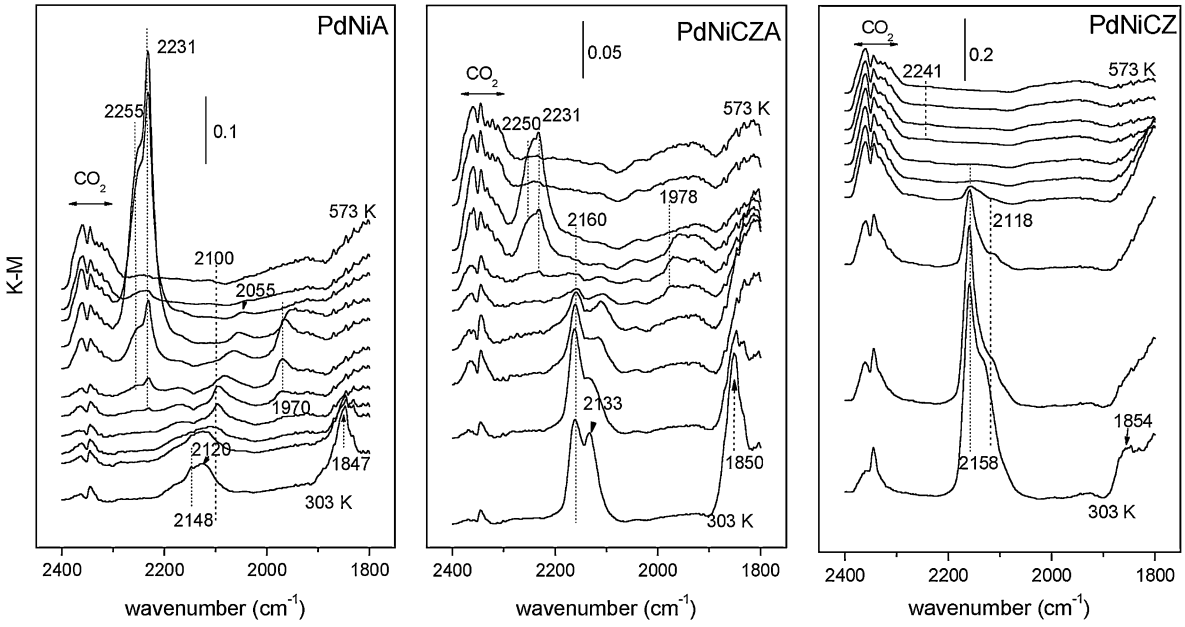

Fig. 4. In situ DRIFTS spectra obtained during the course of the CO–O_2–NO reaction for the indicated catalysts. Spectra taken every 30 K from 303 up to 573 K (from bottom to top).

concentration of NO used in these tests prevents direct monitoring from analysis of the NO gas phase bands in the DRIFTS spectra. Nevertheless, on-line chemiluminescence monitoring of NO_x species during the CO + O_2 + NO reaction revealed good agreement between NO conversion results obtained in the catalytic tests of Fig. 2 and those obtained using the DRIFTS cell. The DRIFTS spectra revealed the formation of different chemisorbed carbonyl (or nitrosyl) species on interaction with the reactant mixtures. Their characteristics and evolution were observed to depend on various factors, including the presence or absence of NO in the mixture and the amount of CZ component present in the catalyst.

Results for the CO + O_2 reaction show the formation of an atop carbonyl species chemisorbed on metallic Pd particles immediately on contact with the reactant mixture at room temperature (band at 2100–2060 cm^{-1}; see Fig. 3) [7,16–19]. Differences in the intensity and frequency of this type of carbonyl species as a function of the presence or absence of CZ in the catalyst are apparent. Whereas for PdNiCZ, maximum intensity of these species was observed immediately on contact with the reactant mixture at 303 K, decreasing in intensity and red-shifting at higher reaction temperature, for PdNiA the maximum appeared at an intermediate reaction temperature (ca. 383 K), showing decreasing intensity along with red-

shifting at higher temperatures. Of significance was the correlation between the onset temperatures of the red shift of this species and the CO oxidation activity, in agreement with previous results for alumina-supported palladium systems [7]. The PdNiCZA system represents an intermediate case, because it shows maximum intensity of the atop species at 303 K, whereas the band appears to be split into two components at intermediate reaction temperatures (at least up to 423 K) as a consequence of the varying extent of perturbation. Analysis of the shifted component in this sample shows fairly similar positions as those observed for PdNiCZ. The band splitting is a consequence of the presence of two types of palladium species interacting with the two different support components, CZ and A, in agreement with results presented in Part 1 [1].

The spectra show also the growth (up to a certain, relatively high, intermediate temperature) of bands due to two different bridging (or bridging and three-fold coordinated, respectively) carbonyls chemisorbed on metallic palladium (bands at ca. 1970 cm^{-1} and a broader one centered at ca. 1920 cm^{-1} and extending down to ca. 1800 cm^{-1}, respectively) [7,16–20]. A decrease in intensity along with a red shift of bands due to this type of carbonyl, likely related mainly to thermal desorption effects, was produced at high temperature. The decreasing atop/bridge carbonyl intensity ratio observed with increasing reaction temperature can be related in part to the increasing size of the Pd metallic particles produced during the course of the reaction [7,21,22]. (Different thermal stabilities should be also considered [17,19,20].) Indeed, this agrees with the fact that evolution of the overall intensity of metallic palladium carbonyl species in PdNiA (Fig. 3) reflects that the degree of palladium reduction increases with reaction temperature. In situ XANES results presented later in this report are also in agreement with a gradual palladium reduction process during the course of the reaction.

Another carbonyl species detected during the runs under $CO + O_2$ corresponds to carbonyl species chemisorbed at oxidized Pd^{n+} sites (band at ca. 2148–2142 cm^{-1}) [10,20], observed exclusively (at relatively low reaction temperatures) for the CZ-containing catalysts (Fig. 3). Careful inspection of the spectra also reveals the presence of a small band at ca. 2180 cm^{-1} at low reaction temperatures that was not detected during similar runs performed using the monometallic Pd systems [7,9]. This band is most likely related to carbonyls weakly chemisorbed at exposed Ni^{2+} cations present in the NiO-type oxide that is highly dispersed on the catalyst [1,23].

To analyze the state of the catalyst at the end of the runs under $CO + O_2$, the samples were cooled under N_2 before CO (3% CO in N_2 flow) was admitted into the DRIFTS cell at 303 K, then purged under N_2 at the same temperature. The results of these experiments are given in Fig. 5. The spectra show the presence of the linear and bridging carbonyl species on the metallic palladium particles, carbonyl species chemisorbed on Pd^{n+} for the CZ-containing catalysts, and the band due to weakly adsorbed carbonyls on Ni^{2+} cations at ca. 2180 cm^{-1}, which readily disappears on N_2 purging. Note that the ratio of the intensities of atop and bridging carbonyls chemisorbed on metallic palladium was particularly high for the PdNiCZ catalyst, whereas PdNiCZA and PdNiA showed greater similarities in this respect. This is in line with the smaller palladium particle size in the final state of the PdNiCZ system, in agreement with the greater dispersion of palladium observed in the characterization results of Part 1 [1,21,22].

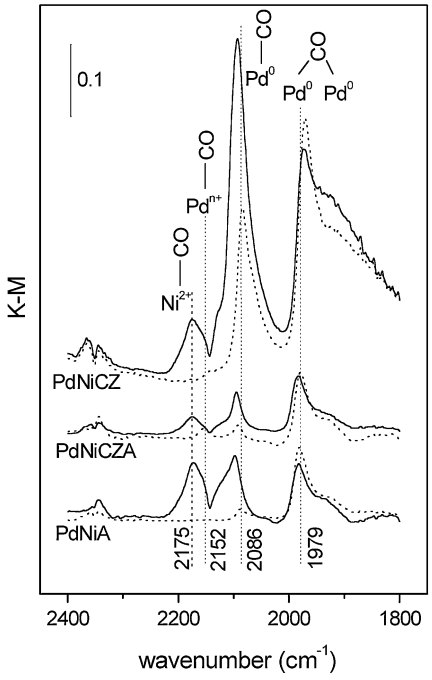

Fig. 5. DRIFTS spectra recorded at the end of the run under $CO–O_2$ after cooling down to 303 K under inert gas followed by admission of 3% CO/N_2 flow (—) and subsequent purging under N_2 (- - -) for the indicated catalysts.

The presence of NO in the reactant mixture significantly hindered the formation of metallic Pd carbonyls (bands at 2100–2060 and 1975–1900 cm^{-1}), as can be inferred by comparing Figs. 3 and 4. In turn, such a comparison reveals that the formation of Pd^{n+} carbonyls (bands at ca. 2160 and 2130 cm^{-1}) was promoted by the presence of NO (Fig. 4). The extent of this effect apparently increased with an increasing amount of CZ in the catalyst. Indeed, for PdNiCZ, it became particularly difficult to detect metallic Pd carbonyls during the temperature ramping. These observations provide evidence of a CZ-promoted oxidizing effect induced by NO on the palladium component, in line with results reported for the monometallic palladium catalysts [10]. Other bands observed in these spectra were related to adsorbed isocyanate species (at ca. 2250 and 2231 cm^{-1} for A-containing catalysts and a very weak one at ca. 2241 cm^{-1} for the PdNiCZ system [7,10,18]), providing evidence for NO dissociation. The initial appearance of these bands correlates reasonably well with the onset of NO reduction. In addition, a band at ca. 1850 cm^{-1} appearing exclusively in the presence of nickel (also seen when the same experiment was performed using a reference Ni/Al_2O_3 catalyst [results not shown]) was observed at relatively low reaction temperatures and can be assigned to nitrosyl species chemisorbed on Ni^{2+} cations [24,25]. Formation of this species hindered formation of the carbonyl species chemisorbed on Ni^{2+} cations, in agreement with the higher adsorption energy of NO over such cations [26]. Re-

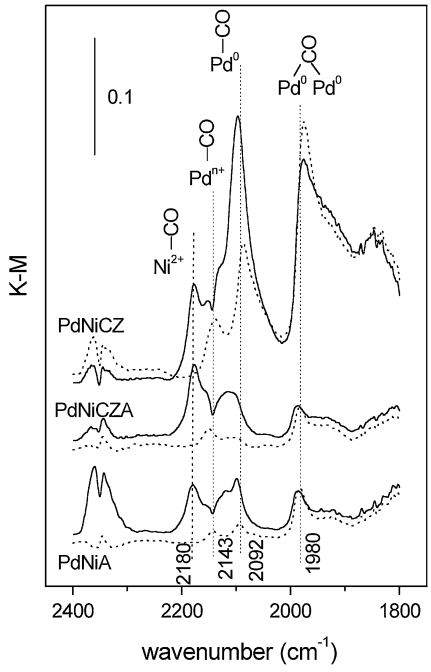

Fig. 6. DRIFTS spectra recorded at the end of the run under CO–O_2–NO after cooling down to 303 K under inert gas followed by admission of 3% CO/N_2 flow (—) and subsequent purging under N_2 (- - -) for the indicated catalysts.

sults (similar to those presented in Fig. 5) of the postreaction chemisorption of CO after the runs under CO + O_2 + NO are displayed in Fig. 6. The nature of the carbonyls detected is similar to that of those observed after the run under CO + O_2. However, a relatively higher intensity of Pd^{n+} carbonyls was detected after the runs under CO + O_2 + NO, indicating that they are apparently favored for CZ-containing catalysts. However, in contrast to results observed after the CO + O_2 run (Fig. 5), a small band due to this type of species was also detected for the PdNiA catalyst in this case. In turn, analysis of the metallic palladium chemisorbed atop/bridge carbonyl intensity ratio is in agreement with the achievement of a smaller palladium particle size in PdNiCZ after the runs under CO + O_2 + NO.

Analysis of the spectral range corresponding to chemisorbed CO_x- or NO_x-related species (assignments made on the basis of differences between experiments performed in the presence and absence of NO) revealed differences as a function of the support material used (Fig. 7). PdNiCZ showed the presence of bands attributable to carbonate or carboxylate species (bidentate carbonates at ca. 1580 and 1297 cm^{-1} and monodentate carbonates or carboxylates at ca. 1506, 1400, and 1332 [27]). A band due to chelating-nitrite species (appearing at 1185 cm^{-1} [28]) was observed at low temperature and had a maximum at 333 K. The evolution of this feature correlates well with the previously mentioned adsorption/desorption phenomena which was responsible for the shape of the NO conversion profile at low temperature during the catalytic tests (Fig. 2). Nitrate species, displaying main bands at 1527 and 1273 cm^{-1} [29–31], are observed at higher reaction temperatures. PdNiA and PdNiCZA catalysts showed the formation of hydrogencarbonate bands (at 1655, 1438, and 1227 cm^{-1} [32,33]) and a band at 1546 cm^{-1} that can be ascribed to a bidentate carbonate species (a band similar to this one is observed to grow with increasing reaction temperature under CO + O_2), although nitrate species could also contribute to this band [33]. Bands attributable to nitrate species (at 1560 and 1308 cm^{-1} [29,33]) are observed at low reaction temperature whereas other types of nitrate species (bands at 1610, 1578 and 1460 cm^{-1} [29,33]) appear at relatively high temperatures. The presence of nickel does not apparently produce significant differences in the nature or evolution of these species, on the basis of comparison with results reported for the monometallic Pd catalysts [7,34]. The carbonate- and nitrate-type species detected in these catalysts are similar to those

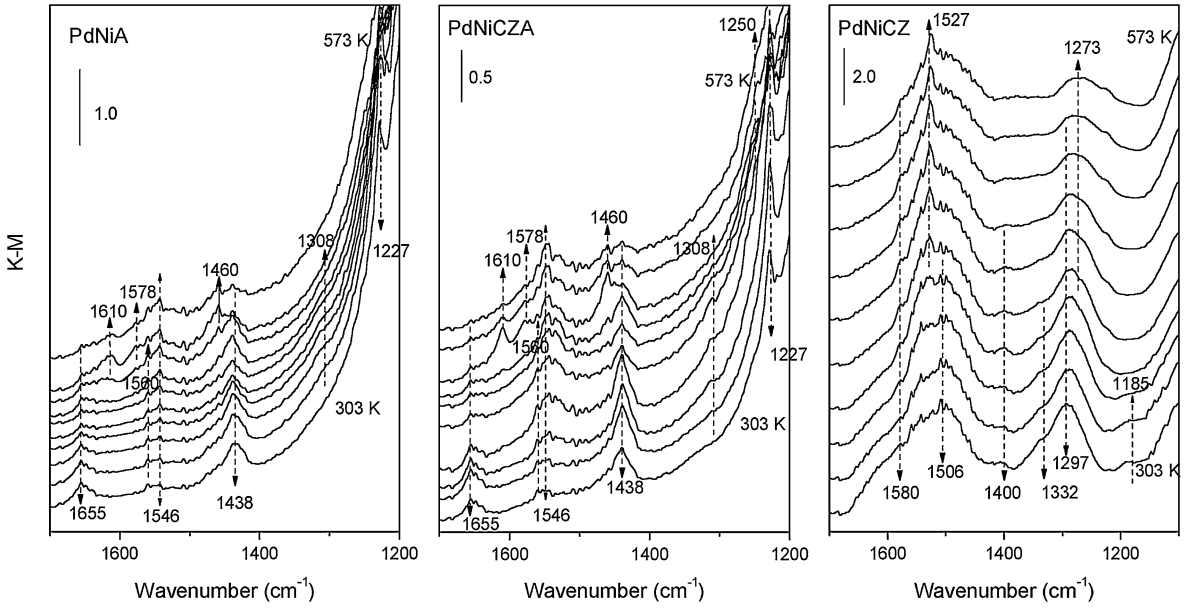

Fig. 7. In situ DRIFTS spectra obtained during the course of the CO–O_2–NO reaction for the indicated catalysts (zone corresponding to carbonate- or nitrate-type species, see text). Spectra taken every 30 K from 303 up to 573 K (from bottom to top).

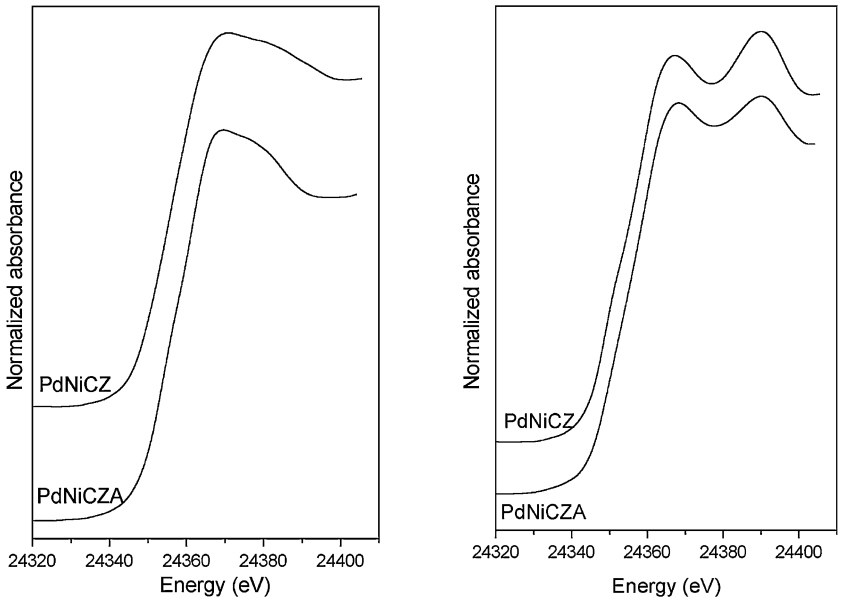

Fig. 8. XANES spectra for the indicated catalysts. (Left) Pd initial, oxidized species; (right) Pd final, reduced species (see text for details).

observed in the metal-free supports and in samples with other metals deposited over these supports [31,33,35], thus indicating that they become stabilized at support surface sites free from significant interactions with either the palladium or nickel components. In turn, their evolution as a function of the reaction temperature, along with comparison with the respective catalytic activities observed for the samples (Figs. 1 and 2), would eliminate any major relevant catalytic role for this type of species, in accordance with previous reports [7,31].

3.3. *In situ* XANES

With the aim of analyzing changes in the chemical state of palladium in the course of the runs under $CO + O_2 + NO$, including the possibility that formation of Pd–Ni alloys may occur under such conditions (as observed previously for analogous Pd–Cu catalysts [3,4]), the two catalysts in which nickel induces apparent changes in catalytic activity were explored by XANES spectroscopy. Principal component analysis (PCA) of the Pd *K*-edge XANES spectra of PdNiCZA and PdNiCZ under $CO + O_2 + NO$ suggested the presence of only two different chemical species during the course of the runs (Fig. 8). Comparing the XANES spectra of the two species with reference compounds indicates that the palladium appears to be present initially in the form of an oxidized Pd^{2+} species with a local symmetry similar to that exhibited by PdO (D_{2h} symmetry group). The second Pd-containing species can be readily ascribed to a zero-valent Pd^0 fcc phase by comparison with a Pd foil. Fig. 9 shows the evolution of the fraction of each of these species as a function of the reaction temperature. The concentration of the Pd^{2+} species decreased gradually from ca. 360 and 410 K for PdNiCZ and PdNiCZA, respectively. The reduced Pd^0 species appear concurrently, and their concentrations then grows until the reduction process becomes complete at about 580 and 630 K, respectively. These results reveal a greater facility for bulk reduction of palladium in the PdNiCZ catalyst.

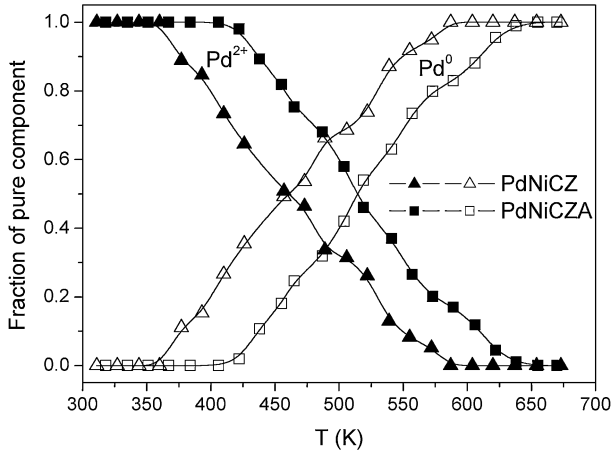

Fig. 9. Concentration profiles of species detected by XANES during the run under $CO–O_2–NO$ for the indicated catalysts.

This can be related to the CZ-promoted reduction of palladium on interaction with CO, in agreement with previous postulations [9,36]. Such a process can in turn be favored by the higher palladium dispersion in this sample [1].

4. Discussion

Promoting effects of nickel in the bimetallic Pd–Ni systems have been shown to depend strongly on the nature of the support used (Table 1). According to earlier reports, [2,7,9,10], such differences must be linked primarily to a series of factors which in general terms can involve morphologic/structural or electronic modifications to palladium and/or the CZ active components of the systems, as well as changes in the nature or the amount of contacts between both active components (as a consequence of changes in the palladium distribution over the supports). Results given in Table 1 discount significant direct involvement of nickel or alumina components on the catalytic activity, although

these components may be indirectly involved by inducing modifications in any of the properties mentioned. In turn, differences as a function of the reactant mixture used in each case must be related to the way in which such different conformations of active components operate with respect to interference between reactants or self-poisoning effects due to deactivation induced on interactions among chemisorbed species [10].

On this basis, the absence of promotional effects of nickel in the PdNiA catalyst indicates that NiO-type species present in the system, according to XPS and XANES results presented in Part 1 [1], do not induce modifications in the characteristics of the active palladium particles and are not involved in phenomena of reactant chemisorption that could affect the catalytic activity of palladium. This latter finding agrees with the limited influence of the nickel entities on the formation of NO- or CO-derived chemisorbed species at temperatures relevant for the catalytic activity, according to the results described earlier. In fact, only weakly chemisorbed carbonyl or nitrosyl species appearing at low temperature could be identified as directly related to the presence of nickel in the catalysts. Such species certainly would not be expected to play a significant role in aspects that could induce important catalytic changes, like producing a modification of the characteristics of the reactant mixture at a local level or activating the reactants in any sense. It must be noted, however, that direct comparison with results of Yamamoto et al. [5,6], who claimed an involvement of nickel species in chemisorption phenomena that could facilitate the palladium activity for this type of reaction [6], yields limited information because of at least two physicochemical differences related to the Ni component. First, their catalyst configuration appears to present nickel fully in the form of a nickel aluminate, according to XRD evidence. In contrast, a mixture of highly dispersed NiO- and $NiAl_2O_4$-type entities is apparently present in the catalysts examined in this work [1]. Second, we use a considerably lower amount of nickel, because in fact optimum properties for the reactions examined here are apparently achieved for such low nickel loading (Table 1). But possible influences of nickel on palladium at structural/morphologic or electronic levels can be considered as residual in our case, on the basis of XANES (Figs. 8 and 9) and STEM analyses [1]. Therefore, the catalytic properties of the PdNiA catalyst can be assimilated into those of the analogous PdA system, which were examined in detail in a previous study [7]. Briefly, the results observed for the $CO + O_2$ reaction are compatible with the typical Langmuir–Hinshelwood kinetic scheme in which the reaction is initially limited by thermal desorption of CO from the metallic Pd particles whose surface atoms constitute the active centers for the reaction [7,20,37,38]. This is based mainly on the correlation observed between the evolution of the frequency of the atop carbonyl species chemisorbed on metallic Pd particles and the catalytic activity (Fig. 3). Thus the relatively high frequency before reaction onset is due to dipolar coupling effects, which mainly govern the frequency of metallic palladium carbonyls (those corresponding to atop species being most sensitive to coupling) [39] in palladium particles highly covered with CO. The simultaneous triggering of CO oxidation and the red shift of the atop carbonyl reflects that desorption of CO allows the reaction to proceed over the particles by leaving sites free for dissociative oxygen adsorption and further combination of the oxygen atoms with chemisorbed CO molecules [7,37,38]. Within this scheme, the irregularities observed in the CO conversion profile for this catalyst (at temperatures < ca. 440 K, giving rise to a kind of staircase-type shape; see Fig. 1) can be attributed to the increase in the number of active sites resulting from the progressive growth of metallic particles during the course of the reaction (in accordance with DRIFTS results presented in Fig. 3). The inhibiting effect of NO on CO oxidation activity (Table 1) can be correlated mainly with the hindering of metallic palladium carbonyl formation observed in the presence of NO (compare Figs. 3 and 4), indicating the greater difficulty in generating active reduced palladium states at the surface of the particles [7]. In turn, the absence of significant effects of nickel on NO reduction (Table 1) further confirms the similar nature of the metallic palladium particles formed during the course of the reaction for PdA and PdNiA, given the strong structural sensitivity of such a reaction [7,40,41].

In contrast to the A-supported catalysts, the presence of nickel significantly affects the catalytic performance of the CZ-supported system (Table 1). The decreased CO oxidation activity and enhanced NO reduction activity observed for the bimetallic PdNiCZ system with respect to the monometallic PdCZ system, along with the absence of significant nickel-induced electronic modifications of palladium (according to XANES analysis; Figs. 8 and 9), suggest that contacts between Pd and the CZ are to a certain (probably small) extent blocked by nickel entities (most likely in the form of NiO-type species [1]); in fact XPS results presented in Part 1 suggested that some interactions between Pd and Ni components can occur in this catalyst [1]. It must be taken into account that the high CO oxidation activity achieved for PdCZ must be mainly a consequence of the existence of contacts between both catalyst components [2,9]. In the presence of such contacts, the direct participation of interfacial oxide anions at the surface of the CZ support in CO oxidation processes allows the opening up of a new reaction path operating at low temperature (<423 K), which circumvents the CO-inhibiting effects observed in A-supported catalysts [2,9,11]. In turn, NO reduction appears to be strongly inhibited in the presence of such contacts as a consequence of the passivation of the active sites at the surface of metallic Pd particles due to the CZ-promoted formation of oxidized states of palladium (in agreement with DRIFTS results described earlier; see Fig. 4). Such an effect is considered mainly responsible for the poorer response of CZ-supported palladium catalysts toward NO reduction [10], in agreement with results presented in Table 1. On this basis, a certain nickel-induced suppression of the establishment of contacts between Pd and CZ can explain the observed catalytic activity differences between PdNiCZ and PdCZ (Table 1). However, another hypothesis that might explain these results could be related to differences (even if small) in the respective palladium dispersions (i.e., a relatively larger palladium crystallite size in PdNiCZ; in any case, within the context of very highly dispersed states for both systems). Unfortunately,

the similar DRIFTS results observed for both samples (results for the monometallic system available elsewhere [10]) does not allow a distinction between these hypotheses, although it highlights the subtle character of the differences between both systems.

The most striking promoting effects of nickel appear for the CZA-supported catalyst and are particularly reflected in the important improvement in CO oxidation activity observed for PdNiCZA (Table 1). In the absence of appreciable electronic modifications of palladium (according to XANES results; Figs. 8 and 9), the most likely hypothesis to account for this effect must be related to the nickel-induced changes in the palladium distribution over the support. Thus, on the basis mainly of the XEDS results presented in Part 1 [1], it has been observed that the presence of nickel favors the formation of contacts between Pd and CZ components of this system. Interestingly, in contrast to observations in the CZ-supported catalysts, such contacts might not necessarily involve highly dispersed palladium particles, because the particle size of palladium particles appears fairly close to that observed for the A-supported catalysts (on the basis of DRIFTS results discussed earlier and STEM-EELS observations presented in Part 1 [1]). In addition, it must be considered that a part of the palladium must be in contact with the alumina component of the catalyst (according to DRIFTS and STEM-EELS results [1]) but does not participate in the low-temperature CO oxidation activity of this system, in accordance with the absence of frequency shifts for the corresponding atop carbonyl species (Fig. 3). Taking these points into account, the fact that the PdNiCZA catalyst displays a CO oxidation catalytic activity similar to that of PdNiCZ, in which palladium appears highly dispersed and the amount of contacts between Pd and CZ components (even if somewhat damped by nickel entities according to the discussion above) is maximized, indicates an important influence of CZ particle size on such activity. In brief, contacts established between Pd and CZ particles in PdNiCZA (average CZ particle size of ca. 3.5 nm [1]) appear to be appreciably more active for CO oxidation than those present in PdNiCZ (average CZ particle size $\approx$ 5.5 nm [1]). This suggests an important role of Pd–CZ interfacial properties on such activity, as has been proposed for other CZ- or ceria-supported metal catalysts [31,42–44]. Size-dependent differences in the chemical activity of oxide nanoparticles can be related to various factors, as has been discussed previously [45,46]. These factors can include electronic changes (e.g., changes in band gap size or introduction of electronic states within the oxide band gap, redistribution of atomic charges) and structural or geometrical changes (e.g., stabilization of determinate crystalline, or even amorphous, phases, particularly at the oxide surface; changes in the amount or distribution of defects). In the case of ceria-related oxides, it has been observed that decreasing the size of the nanoparticles can decrease the reduction temperature of the oxide [47], in agreement with theoretical predictions [48], and also enhance the electronic conductivity [49,50]. Both aspects can play an important role in the CO oxidation activity of Pd–CZ contacts, taking into account the direct participation of oxide anions of the support in the catalytic process.

Concerning the activity of PdNiCZA when NO is present in the reactant mixture, the data show an important NO-induced inhibition of CO oxidation, stronger than that observed for the PdNiCZ catalyst (Figs. 1 and 2; Table 1). The behavior of PdNiCZA in this respect (and in contrast to PdNiCZ, as discussed earlier) is more representative of the presence of pure Pd–CZ contacts than those present in PdCZ, which also shows a large inhibiting effect of NO [10], Table 1. According to previous studies [10], such an inhibiting effect can be related to the previously mentioned CZ-promoted formation of oxidized states of palladium (according to DRIFTS results), which would impede CO adsorption and activation, and/or to NO interference with oxygen adsorption, leading to reoxidation of interfacial vacancies of CZ [10,28]. However, it is interesting that the PdNiCZA catalyst still maintains a level of NO reduction activity similar to that achieved by the analogous PdCZA reference (Table 1). Because, as mentioned earlier, poorer NO reduction activity would be expected for palladium sites in contact with the CZ component [10], this result suggests a different nature for the sites active for such reaction. In fact, palladium particles in contact with the alumina component are shown to be most active for this reaction (Table 1), whereas interactions of these with highly dispersed two-dimensional CZ entities can also favor such processes [10]. In this sense, no significant particle size differences were apparent for such noble metal particles, in comparison with the other CZA- or A-supported systems of the analogous series, according to the analysis of Z-contrast images [1]. Nevertheless, considering the prevailing interaction between palladium and CZ in this catalyst, the nickel-induced morphologic changes in palladium particles in contact with the CZ component (in particular, achievement of a larger particle size [1]) can also have an important role in the NO reduction activity of this catalyst [2,7].

5. Conclusions

Pd–Ni catalysts supported on Al_2O_3, $(Ce,Zr)O_x/Al_2O_3$, and $(Ce,Zr)O_x$ have been examined with regard to their catalytic activity for CO oxidation and NO reduction under stoichiometric $CO–O_2$ and $CO–O_2–NO$ mixtures, focusing mainly on the effects induced by the presence of nickel on the catalytic activity. These are shown to depend strongly on the support used. Whereas practically no differences are detected for the Al_2O_3-supported bimetallic catalyst in comparison with the analogous monometallic palladium system [7,9,10], apparent differences appear for $(Ce,Zr)O_x$-containing catalysts. Because no apparent modification of the palladium electronic properties (as would be expected on, for instance, formation of alloys with nickel) were detected by in situ XANES experiments, and no direct involvement on the catalytic processes could be attributed to the highly dispersed oxidized nickel entities present in the catalysts [1], the changes observed are related to indirect effects involving modifications in the catalyst configurations with respect to the corresponding monometallic palladium references. The lower CO oxidation and higher NO reduction activities observed for the $(Ce,Zr)O_x$-supported system suggest that active contacts between highly dispersed Pd and $(Ce,Zr)O_x$ are

modified either through direct blocking by NiO-type entities or through a certain decrease in the palladium dispersion. An important promotion of CO oxidation activity is observed for the $(Ce,Zr)O_x/Al_2O_3$-supported catalyst as a result of Ni-induced changes in the palladium distribution over the support, which favors the generation of active Pd–$(Ce,Zr)O_x$ contacts [1]. The significant extent of such a promoting effect reveals an important role of the particle size of the $(Ce,Zr)O_x$ component on such catalytic processes.

Acknowledgments

The authors thank the technical and scientific staff at the ESRF BM-29 (Dr. G. Subías) and SRS 9.3 (Drs. A.R. Lennie and I. Harvey) synchrotron beamlines, and Dr. A. Iglesias-Juez for their help in the recording of XAFS data. They also thank Professor J.C. Conesa for helpful discussions. A.B.H. thanks the Comunidad de Madrid for a doctoral studies grant and for financial support through the "Ayudas para estancias en centros extranjeros" program. Support for this work was also provided by the CICyT (project MAT2000-1467).

References

[1] A.B. Hungría, N.D. Browning, R.P. Erni, M. Fernández-García, J.C. Conesa, J.A. Pérez-Omil, A. Martínez-Arias, J. Catal., in press, 10.1016/j.jcat.2005.08.011.
[2] A. Martínez-Arias, J.C. Conesa, M. Fernández-García, J.A. Anderson, in: J.A. Anderson, M. Fernández-García (Eds.), Supported Metals in Catalysis, Imperial College Press, London, 2005, p. 283.
[3] M. Fernández-García, A. Martínez-Arias, C. Belver, J.A. Anderson, J.C. Conesa, J. Soria, J. Catal. 190 (2000) 387.
[4] A.B. Hungría, A. Iglesias-Juez, A. Martínez-Arias, M. Fernández-García, J.A. Anderson, J.C. Conesa, J. Soria, J. Catal. 206 (2002) 281.
[5] S. Yamamoto, K. Matsushita, Nippon Kagaku Kaishi (2000) 553.
[6] S. Yamamoto, K. Matsushita, Y. Hanaki, Nippon Kagaku Kaishi (2001) 19.
[7] A. Martínez-Arias, A.B. Hungría, M. Fernández-García, A. Iglesias-Juez, J.A. Anderson, J.C. Conesa, J. Catal. 221 (2004) 85.
[8] R. van Yperen, D. Lindner, L. Mubmann, E.S. Lox, T. Kreuzer, Stud. Surf. Sci. Catal. 116 (1998) 51.
[9] M. Fernández-García, A. Martínez-Arias, A. Iglesias-Juez, A.B. Hungría, J.A. Anderson, J.C. Conesa, J. Soria, Appl. Catal. B 31 (2001) 39.
[10] A. Martínez-Arias, M. Fernández-García, A. Iglesias-Juez, A.B. Hungría, J.A. Anderson, J.C. Conesa, J. Soria, Appl. Catal. B 31 (2001) 51.
[11] M. Shelef, G.W. Graham, R.W. McCabe, in: A. Trovarelli (Ed.), Catalysis by Ceria and Related Compounds, Imperial College Press, London, 2002, p. 343.
[12] R. Di Monte, J. Kaŝpar, Catal. Today 100 (2005) 27.
[13] R. Cataluña Veses, Ph.D. Thesis, Universidad Politécnica de Madrid (2005).
[14] M. Fernández-García, Catal. Rev. Sci. Eng. 44 (2002) 59.
[15] C.N. Costa, S.Y. Christou, G. Georgiou, A.M. Efstathiou, J. Catal. 219 (2003) 259.
[16] R. Raval, G. Blyholder, S. Haq, D.A. King, J. Phys.: Condens. Matter 1 (1989) SB165.
[17] X. Xu, P. Chen, D.W. Goodman, J. Phys. Chem. 98 (1994) 9242.
[18] K. Almusaiteer, S.C. Chuang, J. Catal. 184 (1999) 189.
[19] I.V. Yudanov, R. Sahnoun, K.M. Neyman, N. Rösch, J. Hoffmann, S. Schauermann, V. Johánek, H. Unterhalt, G. Rupprechter, J. Libuda, H.-J. Freund, J. Phys. Chem. B 107 (2003) 255, and references therein.
[20] X. Xu, D.W. Goodman, J. Phys. Chem. 97 (1993) 7711.
[21] K. Wolter, O. Seiferth, H. Kuhlenbeck, M. Bäumer, H.-J. Freund, Surf. Sci. 399 (1998) 190.
[22] M. Frank, M. Bäumer, Phys. Chem. Chem. Phys. 2 (2000) 3723.
[23] C. Xu, Q. Guo, D.W. Goodman, Catal. Lett. 41 (1996) 21.
[24] G. Niu, Y. Huang, Z. Cao, Y. Huang, Q. Li, Appl. Surf. Sci. 141 (1999) 35.
[25] J.B. Peri, J. Catal. 86 (1984) 84.
[26] A. Zecchina, D. Scarano, S. Bordiga, G. Ricchiardi, G. Spoto, F. Teobaldo, Catal. Today 27 (1996) 403.
[27] C. Li, Y. Sakata, T. Arai, K. Domen, K.-I. Maruya, T. Onishi, J. Chem. Soc., Faraday Trans. I 85 (1989) 929.
[28] A. Martínez-Arias, J. Soria, J.C. Conesa, X.L. Seoane, A. Arcoya, R. Cataluña, J. Chem. Soc., Faraday Trans. 91 (1995) 1679.
[29] A.A. Davydov, in: C.H. Rochester (Ed.), Infrared Spectroscopy of Adsorbed Species on the Surface of Transition Metal Oxides, Wiley, New York, 1990, p. 75.
[30] K. Hadjiivanov, V. Avreyska, D. Kissurski, T. Marinova, Langmuir 18 (2002) 1619.
[31] A. Martínez-Arias, M. Fernández-García, A.B. Hungría, A. Iglesias-Juez, O. Gálvez, J.A. Anderson, J.C. Conesa, J. Soria, G. Munuera, J. Catal. 214 (2003) 261.
[32] A.M. Turek, I.E. Wachs, E. DeCanio, J. Phys. Chem. 96 (1992) 5000.
[33] A. Martínez-Arias, M. Fernández-García, A. Iglesias-Juez, J.A. Anderson, J.C. Conesa, J. Soria, Appl. Catal. B 28 (2000) 29.
[34] A. Iglesias Juez, Ph.D. Thesis, Universidad Autónoma de Madrid (2005).
[35] A. Martínez-Arias, A.B. Hungría, M. Fernández-García, J.C. Conesa, G. Munuera, J. Power Sources (in press).
[36] M. Fernández-García, A. Martínez-Arias, L.N. Salamanca, J.M. Coronado, J.A. Anderson, J.C. Conesa, J. Soria, J. Catal. 187 (1999) 474.
[37] T. Engel, G. Ertl, Adv. Catal. 28 (1979) 2.
[38] J. Libuda, I. Meusel, J. Hoffmann, J. Hartmann, L. Piccolo, C.R. Henry, H.-J. Freund, J. Chem. Phys. 114 (2001) 4669.
[39] P. Hollins, Surf. Sci. Rep. 16 (1992) 51.
[40] D.R. Rainer, S.M. Vesecky, M. Koranne, W.S. Oh, D.W. Goodman, J. Catal. 167 (1997) 234.
[41] L. Piccolo, C.R. Henry, J. Mol. Catal. A 167 (2001) 181.
[42] J.G. Nunan, H.J. Robota, M.J. Cohn, S.A. Bradley, J. Catal. 133 (1992) 309.
[43] A. Martínez-Arias, A.B. Hungría, M. Fernández-García, J.C. Conesa, G. Munuera, J. Phys. Chem. B 108 (2004) 17983.
[44] S. Carrettin, P. Concepcion, A. Corma, J.M.L. Nieto, V.F. Puntes, Angew. Chem.-Int. Ed. 43 (2004) 2538.
[45] M. Fernández-García, A. Martínez-Arias, J.C. Hanson, J.A. Rodríguez, Chem. Rev. 104 (2004) 4063, and references therein.
[46] R. Di Monte, J. Kaŝpar, J. Mater. Chem. 15 (2005) 633.
[47] J.A. Rodriguez, J.C. Hanson, J.-Y. Kim, G. Liu, A. Iglesias-Juez, M. Fernández-García, J. Phys. Chem. B 107 (2003) 3535.
[48] H. Cordatos, D. Ford, R.J. Gorte, J. Phys. Chem. 100 (1996) 18128.
[49] Y.-M. Chiang, E.B. Lavik, I. Kosacki, H.L. Tuller, J.Y. Ying, J. Electroceram. (1997) 7.
[50] A. Tschöpe, E. Sommer, R. Birringer, Solid State Ionics 139 (2001) 255.